PERGAMON

Journal of Structural Geology 25 (2003) 1795–1813

JOURNAL OF STRUCTURAL GEOLOGY

www.elsevier.com/locate/jsg

Overprinting faulting mechanisms in high porosity sandstones of SE Utah

N.C. Davatzes*, A. Aydin

Department of Geology and Environmental Science, Stanford University, Stanford, CA, 94305-2115, USA

Received 19 March 2002; received in revised form 28 January 2003; accepted 14 February 2003

Abstract

Normal faults in sandstone of the Jurassic Entrada Formation, South-East Utah formed by two mechanisms: (1) deformation band faulting overprinted by (2) jointing and subsequent shearing along joints. Fundamental structural elements of deformation band faults are single deformation bands, zones of deformation bands, and slip surfaces. Joint-based faults are composed of joints, sheared joints, splay fractures, fragmentation zones, breccia, and fine-grained fault rock. We demonstrate that both mechanisms contribute to slip in a single fault zone with joint-based faulting consistently postdating deformation band faulting at a given location along a fault. The occurrence, distribution, and geometric arrangement of structures formed by the two mechanisms resulted in faults with distinct fault architecture. This fault architecture is related to the relative contributions of each deformation mechanism to the total offset and to their relative timing. Overprinting of a deformation band-based fault by a joint-based mechanism introduces extensive localized structural heterogeneity with a distinct hydraulic signature. Whereas deformation bands tend to act as fluid baffles, joints may act as preferred fluid conduits. Therefore, fluid flow properties such as the permeability of the faults with overlapping mechanisms are expected to change over time accompanying the overprinting process.

Keywords: Fault Architecture; Deformation band; Joint; Normal fault; Sheared joint; Sandstone

1. Introduction

Fault localization and slip are products of the deformation mechanisms operating in rocks. In porous sandstone two end-member mechanisms are recognized: deformation banding (Aydin and Johnson, 1978; Antonellini and Aydin, 1994) and shearing across joints/joint zones (Myers, 1999; Flodin, 2003). Each of these mechanisms produces corresponding unique products. The deformation band-based mechanism produces individual deformation bands, zones of deformation bands, and slip surfaces. The sheared joint based mechanism produces joints, sheared joints, zones of fragmentation (volumes of fracture-bounded rock), breccia, and eventually fine-grained fault rock (gouge). Previously, each of these mechanisms has been described in isolation in order to develop conceptual models of fault growth in simple cases of small offset. In this paper, we examine faults formed by contributions from both mechanisms and the resulting variation in the fault zone architecture.

Cataclastic deformation band formation in porous sandstone involves pore collapse and grain-fracturing, resulting in a tabular zone of localized shear strain. Deformation bands with cataclasis typically occur in host rock where initial porosity exceeds ~15% (Antonellini and Aydin, 1994). Field studies (Engelder, 1974; Aydin and Johnson, 1978; Jamison and Stearns, 1982; Antonellini et al., 1994; Davis, 1999) and laboratory experiments (Wong et al., 1997; Mair et al., 2000) demonstrate that single deformation bands accommodate a consistent amount of shear strain on the order of unity. Both field (Aydin and Johnson, 1978) and laboratory (Mair et al., 2000) studies show that additional shear is accommodated by formation of new deformation bands. Aydin and Johnson (1978) proposed a conceptual model for the progressive development of faults in porous sandstone by the 'deformation banding mechanism' that includes the successive development of a single deformation band, a zone of deformation bands, and a slip surface adjacent to a zone of deformation bands (Fig. 1a).

The sheared joint mechanism is characterized by an initial stage of opening mode fracturing followed by shear localization on the initial fractures (Fig. 1b). Jointing and subsequent shearing along joints may occur as separate events or as part of the same deformation episode (Barton,

* Corresponding author.
E-mail address: davatzes@pangea.stanford.edu (N.C. Davatzes).

0191-8141/03/$ - see front matter © 2003 Elsevier Ltd. All rights reserved.
doi:10.1016/S0191-8141(03)00043-9

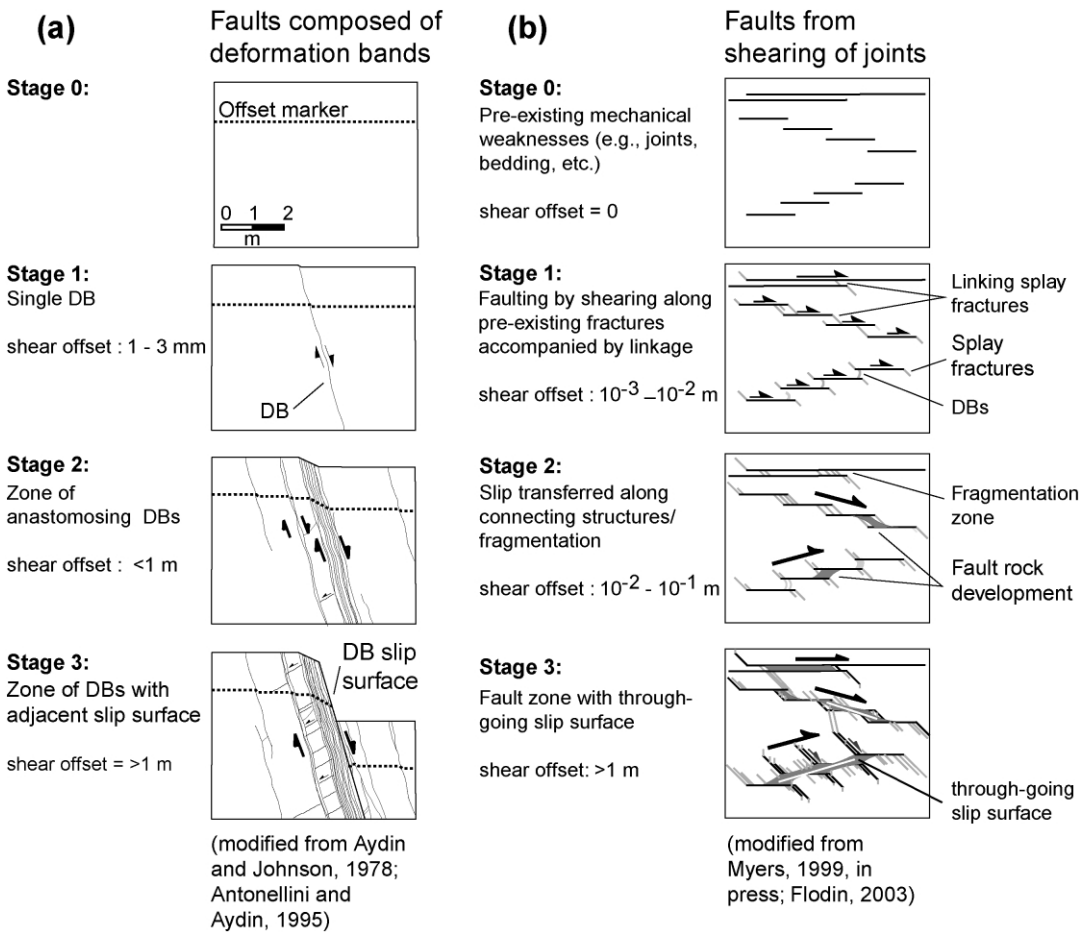

Fig. 1. (a) Stages of deformation beginning with a single deformation band (DB). At latter stages, as zones of DBs develop, new DBs at an angle to the primary set may form. Modified from Aydin and Johnson (1978) and Antonellini and Aydin (1994). (b) Stages of fault development by the sheared joint deformation mechanism. (Figure after Davatzes et al. (2003).)

1983; Dyer, 1983; Cruikshank et al., 1991a,b; Zhao and Johnson, 1992; Wilkins et al., 2001). Shearing across joints produces dilatational quadrants in which new joints may form at or near the tip of the sheared joints (Segall and Pollard, 1980). The new generation of joints is collectively known in the literature as splay fractures, secondary fractures, horsetail fractures, pinnate fractures, kink fractures, bridge fractures, and tail fractures (Segall and Pollard, 1980; Granier, 1985; Engelder, 1987; Martel, 1990; Cruikshank et al., 1991a; Cruikshank and Aydin, 1994). Splay fractures have also been recognized as a result of slip on planar discontinuities such as dune boundaries (Cooke, 1997) and stylolites (Fletcher and Pollard, 1981; Willemse and Pollard, 1998).

Experiments that explicitly include macroscopic joints subjected to shear deformation verify that new fractures form at the periphery of the sheared discontinuities (Brace and Bombolakis, 1963; Peng and Johnson, 1972; Nemat-Nasser and Horii, 1982) or at bridges between en échelon sheared joints (Lin and Logan, 1991). Multiple splay fractures may be expected due to spatially varying friction (Gentier et al., 2000) and associated with high slip gradient (Cooke, 1997; Willemse and Pollard, 1998). These locations become pockets of intense fragmentation (Cruikshank and Aydin, 1994; Myers, 1999). As slip increases, joints that initially formed as splay fractures slip and form a second generation of splay fractures. The formation of multiple generations of splay fractures fragment the rock adjacent to a slipping surface (Flodin, 2003; Myers, 2003) leading to the formation of breccia. Segall and Pollard (1983), Martel et al. (1988), Dholakia et al. (1998), and Myers (1999) proposed a conceptual model for the progressive development of faults by the successive development of joints, sheared joints, new joints as splay fractures, rock fragments, breccia, and fault rock.

These two mechanisms may occur in the same rock at the same place, thereby producing overprinting, complex structural patterns. The products of an earlier deformation mechanism can greatly influence the distribution of subsequent deformation by creating physical discontinuities and introducing strong anisotropy. Several studies demonstrate that pre-existing tectonic structures act as a control on the occurrence and distribution of subsequent deformation. In Arches National Park, Utah joints form along pre-existing deformation bands (Cruikshank et al., 1991a,b; Antonellini and Aydin, 1995). Hence, the spacing and orientation of

deformation bands potentially affect joint orientation and spacing. Roznovsky and Aydin (2001) reported a similar case in the Navajo sandstone in Capitol Reef National Park. Deformation bands may form as a result of compression localized between slipping en échelon joints. Conversely, joints may also form as splay fractures in the dilatational quadrant of a sheared discontinuity (Dyer, 1983; Segall and Pollard, 1983; Cruikshank and Aydin, 1994; Ohlmacher and Aydin, 1993) resulting in a more intricate spatial and temporal relationship among the structural components of a fault. Finally, because joints create pathways of connected pore space, they tend to act as preferred fluid conduits (Dholakia et al., 1998). Furthermore, slight shearing enhances the permeability of a sheared joint (Taylor et al., 1999). In contrast, deformation bands create zones of porosity loss that can potentially impede fluid flow (Antonellini and Aydin, 1994; Matthäi et al., 1998). Therefore, fault zones composed of overprinting fundamental structural elements respond differently to fluid flow in both fault parallel and fault perpendicular directions before and after the overprinting.

We demonstrate that the geometry, distribution and relative timing of the corresponding structural products can be distinguished and mapped along an exposed fault trace or cross-section. This information establishes (1) the architecture of the fault, (2) the deformation mechanisms involved in fault formation, (3) the interaction of different mechanisms to accommodate deformation in the fault zone, and (4) the history of fault development and slip. Because different mechanisms involve different structural components and produce different fault architectures, distinguishing their occurrence and role in faulting is a necessary first step in understanding fault zone development and their hydraulic properties.

We document the occurrence of different structures associated with normal faults and partition their contributions to the total throw in order to quantify the effects of two different deformation mechanisms on fault architecture and slip. We demonstrate that the resulting distribution of offset and the spatial arrangement of structures composing the fault zone and damage zone result from two overprinting deformation mechanisms. We propose that variation in the relative abundance of the structures composing a fault zone may be directly related to the proportion of offset accommodated by each deformation mechanism.

We studied normal faults in the Jurassic Moab Tongue Member and Slick Rock Member sandstone units in the northeastern Paradox Basin of Utah (Fig. 2). We focus on faults with throw ranging from 3 to 140 m. Examining faults over a range of offset provides the opportunity to elucidate the progressive development of faults and their architecture with reference to overlapping faulting mechanisms.

2. Geologic setting

2.1. Regional Paradox Basin

The Paradox Basin is defined by a thick Pennsylvanian evaporite unit known as the Paradox Formation (Fig. 3). Movement of the salt following deposition (Fig. 4) is evident in the thickness distribution, local non-deposition, (Doelling, 1988) and internal sedimentary structure of several units overlying the Paradox Formation. Both phenomena are the result of anticline/syncline formation resulting from salt redistribution and flexure of overlying rock. Data were collected in two locations within the northeastern Paradox Basin (Fig. 2a).

2.2. Faults in Cache Valley in Arches National Park

Cache Valley is located along the eastern border of Arches National Park, Utah (Fig. 2b). A salt diapir developed below Cache Valley during the period of greatest salt movement from the Pennsylvanian through the Triassic (Fig. 4) (Cater, 1970; Dyer, 1983; Doelling, 1988). This diapir folded overlying strata to form a salt anticline. Continued diapirism was probably responsible for producing the faults bounding Cache Valley during the Tertiary (Dyer 1983; Doelling, 1985). Most recently salt dissolution may have contributed to slip on these faults (Doelling, 1988; Oviatt, 1988). These bounding faults offset Jurassic through at least Triassic rocks and probably penetrate into the Pennsylvanian Paradox Formation.

Data were collected along two linked normal fault segments and a series of small faults exposed in aeolian Jurassic Moab Tongue sandstone of the Entrada Formation pavement surface in Cache Valley (Fig. 2b). The measured fault dip varies from 72° to near vertical, averaging 75°. Slickenlines observed along the fault trace indicate nearly pure normal slip with an average observed rake of 88° from the west. These two faults overlap and are linked with a combined length of 1400 m (Fig. 5). The maximum offset exceeds 55 m just west of the linkage.

The Moab Tongue is characteristically calcite cemented, fine to medium grained, well-sorted quartz arenite with low angle cross-stratification (Doelling, 1988; Foxford et al., 1996). In the park the unit is 20–40 m thick. The thickness decreases slightly near the crest of salt anticlines and increases into adjacent synclines (Doelling, 1996) indicating topography resulting from active salt movement during deposition. Average reported porosity of the Moab Tongue sandstone in the park is 18–25% (Dyer, 1983; Antonellini and Aydin, 1994, 1995).

2.3. Faults in the Spanish-Moab Valley

The Moab fault is a 45-km-long normal fault with up to 1000 m vertical stratigraphic offset (Doelling, 1985; Foxford et al., 1996) in the Spanish Valley (Fig. 2c). The

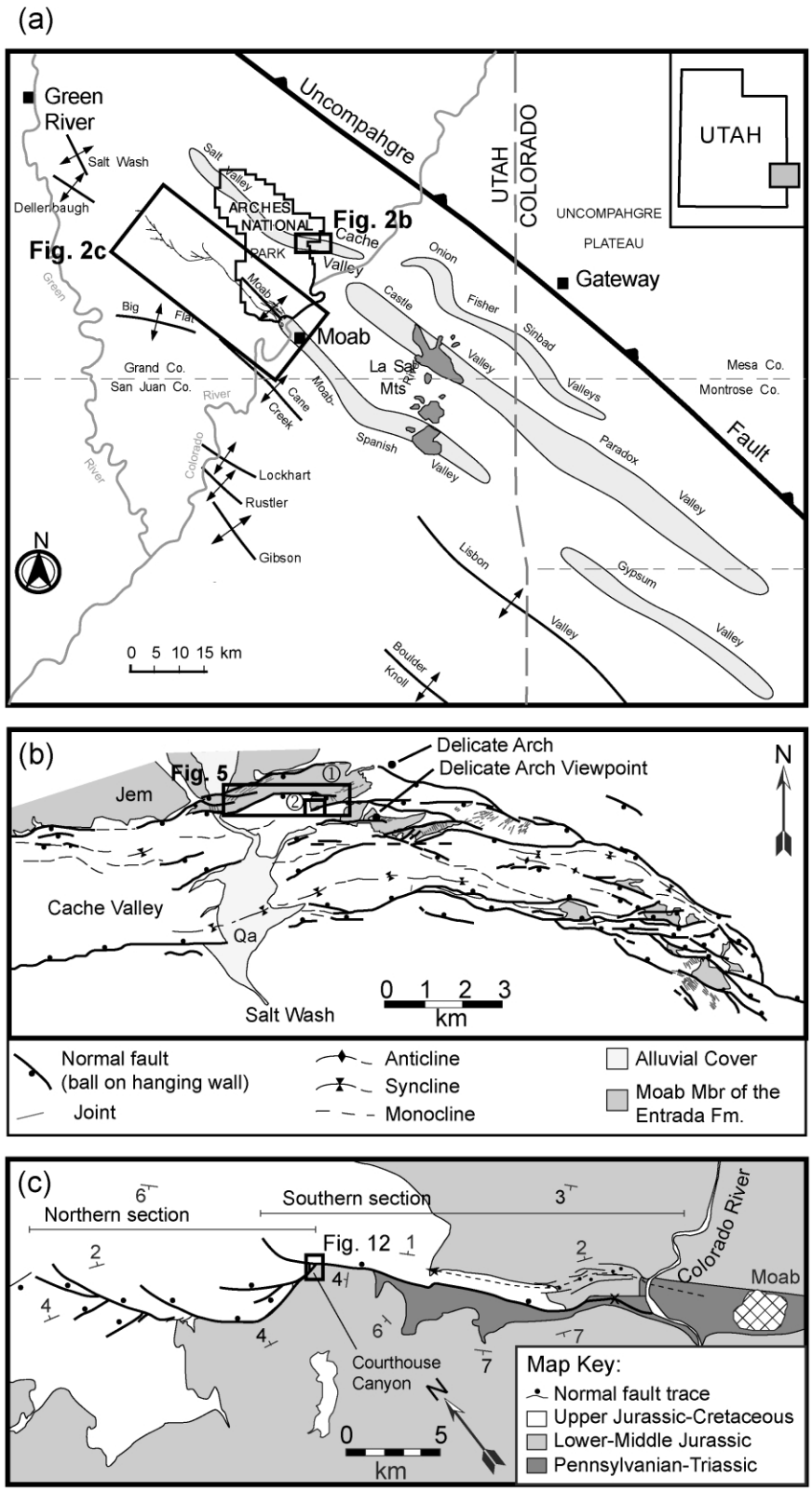

Fig. 2. Location maps of study sites within the Paradox Basin, east central Utah. (a) The study areas lie above the deepest part of the basin and the location of greatest initial Paradox salt thickness and active salt movement leading to salt anticline formation. (Modified from Doelling, 1988) (b) Tectonic map of Cache Valley. Faults trend predominantly sub-parallel to the axis of the Cache Valley salt-cored anticline (Doelling, 1988). Boxes 1 and 2 indicate areas of study and Figs. 6 and 8, respectively. (Modified from Antonellini and Aydin, 1995) (c) Tectonic map of the Moab fault. Location of maximum offset is marked as 'X'. The Courthouse Canyon study area is boxed. Modified from Foxford et al. (1996) and Doelling (1985).

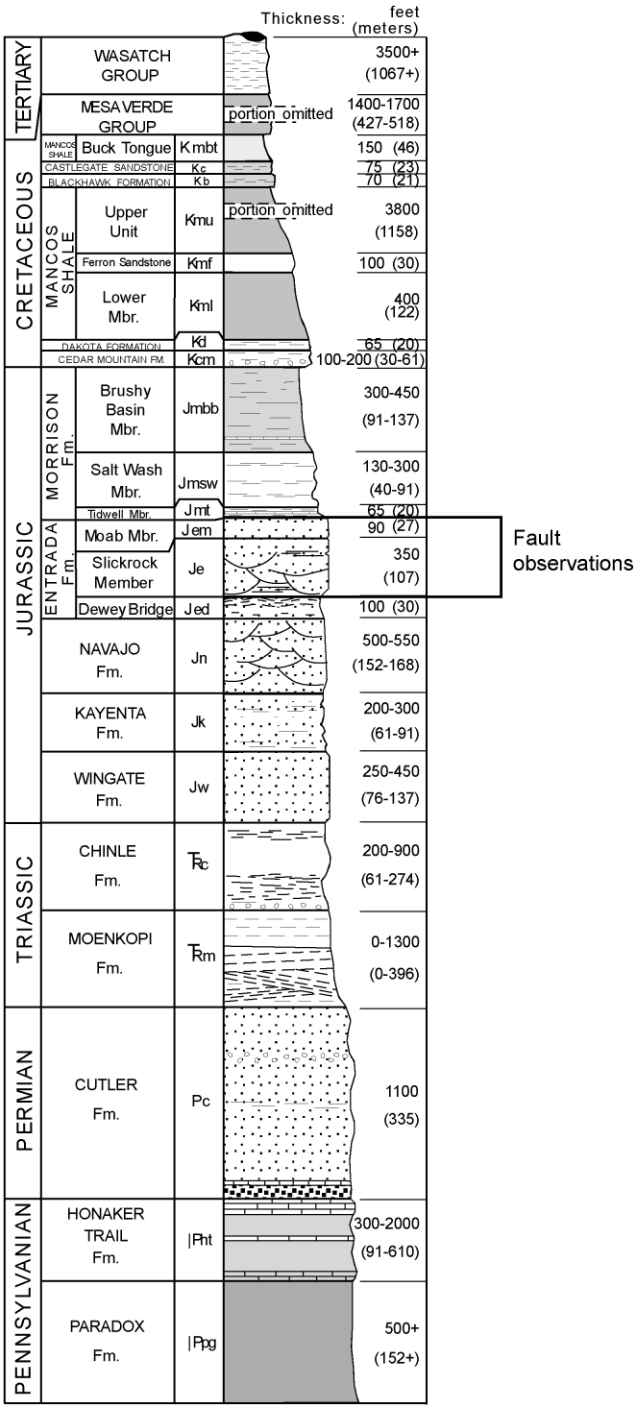

Fig. 3. Stratigraphic column showing units outcropping in the study area (modified from Doelling (1985)). An undetermined thickness of Tertiary rock has been eroded during uplift of the Colorado Plateau. Note that the Jurassic Entrada Sandstone and its Moab Tongue and Slick Rock Members are marked.

fault is spatially associated with a salt-cored anticline (Fig. 2). Pennsylvanian through Cretaceous sandstone and shale (Fig. 3) offset by the fault are exposed along the trace (Doelling, 1985). Late Cretaceous and early Tertiary rocks have been eroded from both hanging wall and footwall accompanying uplift of the Colorado Plateau.

Data were collected in the Courthouse Canyon that intersects the Moab fault at a high angle. The canyon walls are composed of the Dewey Bridge, Slick Rock, and Moab Tongue Members of the Entrada sandstone (Fig. 2c) in the footwall of the Moab fault. Small faults related to the Moab fault are examined in the cross-section of Slick Rock sandstone along the canyon walls.

The Slick Rock Member of the Entrada sandstone is an aeolian dune sand inter-bedded with laminated muddy siltstone sabkha beds. Siltstone beds form extensive horizontal boundaries within the unit tens to hundreds of meters wide. The sandstone is fine to medium grained, well-sorted with porosity from 14 to 23% (Dyer, 1983; Antonellini and Aydin, 1994, 1995; Foxford et al., 1996). The sandstone is dominantly silica cemented with local calcite cement and veins. The Slick Rock derives a reddish color from hematite staining that is locally bleached by later reducing fluids (Foxford et al. 1996).

Faulting in this location probably occurred between 60 and 43 Ma (Fig. 4) based on K–Ar dating of fine-grained illite within the shale gouge in the Morrison Formation (Pevear et al., 1997). This faulting event was associated with a period of salt movement (Doelling, 1988) and took place during maximum burial of the Entrada Formation at about 2200 m (Pevear et al., 1997; Garden et al., 2001) or during a phase of subsidence immediately preceding maximum burial (Nuccio and Condon, 1996, 1999; Garden et al., 2001). Joints spatially associated with the fault also demonstrate localized calcite and iron oxide cement, reduction haloes, and bitumen that suggest that the joints may have formed while the fault was active from 60 to 43 Ma (Foxford et al., 1996; Chan et al., 2000; Garden et al., 2001). Hence joints are older than these diagenetic events.

3. Methods

In this paper, fault architecture refers to the type, geometry, distribution and density of structures composing the fault and damage zones. The architecture defines the spatial relationships of characteristic structural components. We used two basic methods to quantify the fault architecture. First, field identification of structures such as deformation bands, zones of deformation bands, joints, sheared joints, splay fractures and breccia established categories that were distinguished during mapping. We used either photographs or detailed topographic maps overlain by a 1-m grid for detailed mapping. Larger scale mapping was facilitated by use of the global positioning system (differential GPS). Second, the frequency, orientation and crosscutting relationship of each category of structure and their contribution to offset were measured along scan-lines oriented normal to the fault trace and binned into 1-m intervals. Scan-line length was determined for each case to extend beyond the damage zone (Caine et al., 1996; Knipe, 1997) of the fault into a region where

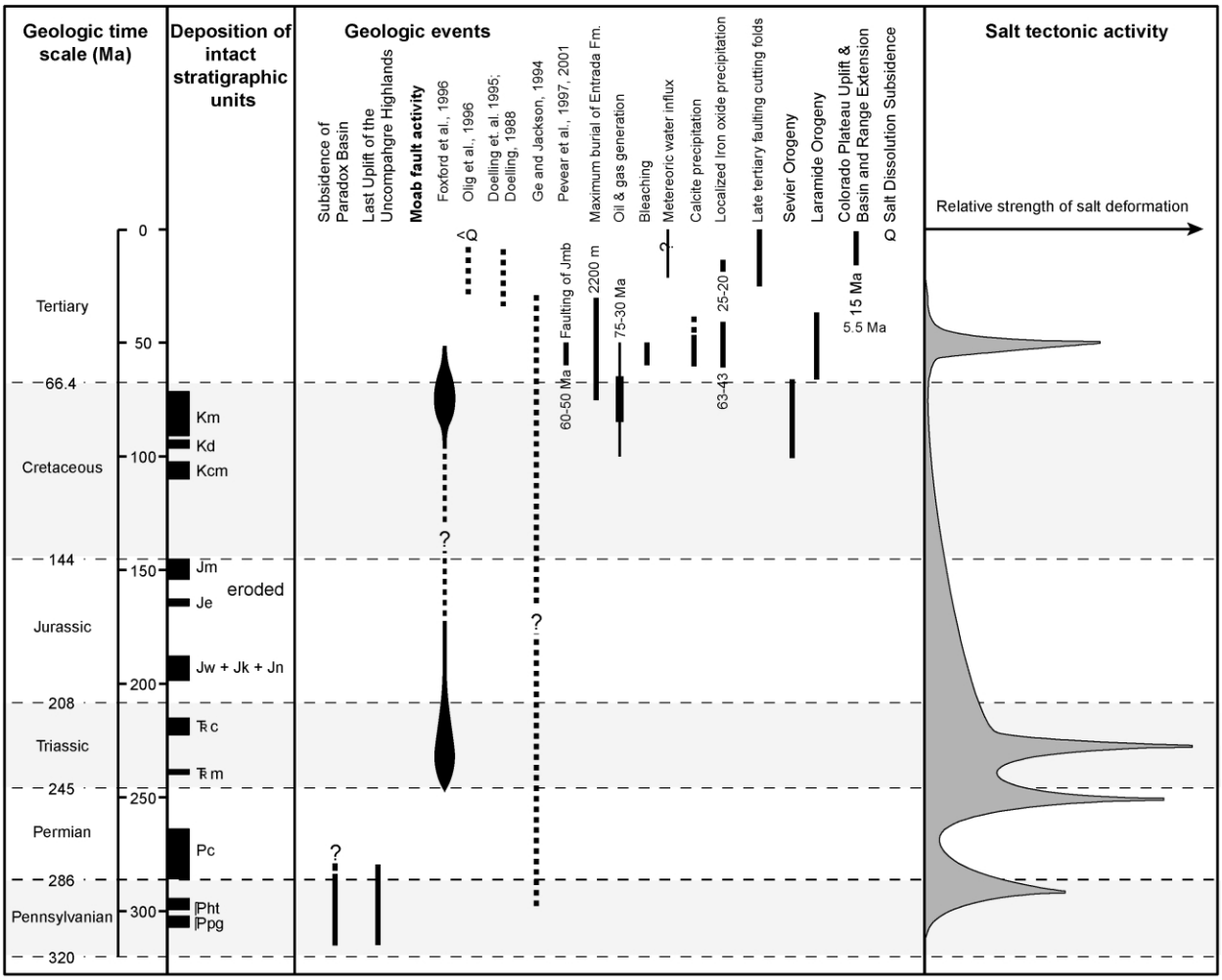

Fig. 4. Compiled information for geologic events and their timing in the study area. The sources are: deposition of lithologic units (Molenaar, 1987; Hintze, 1988); Moab fault activity (Doelling, 1985, 1988; Ge et al., 1994; Olig et al., 1996; Foxford et al., 1996, 1998; Pevear et al., 1997; Vrolijk et al., 1999); maximum burial of Entrada Fm. (Nuccio and Condon, 1996, 1999; Garden et al., 2001); oil and gas generation (Nuccio and Condon, 1996, 1999) with following oil migration into study area (Garden et al., 2001); bleaching (reducing event) (Garden et al., 1997, 2001; Chan et al., 2000); meteoric water influx (Foxford et al., 1996; Pevear et al., 1997; Vrolijk et al., 1999; Chan et al., 2000); calcite precipitation (Garden et al., 2001); localized iron oxide precipitation (Foxford et al., 1996; Chan et al., 2000, 2001); Late Tertiary faulting cutting folds (Doelling, 1988; Friedman et al., 1994); Laramide and Sevier orogenies (Hintze, 1988); Colorado Plateau Uplift (Hunt, 1969; Lucchitta, 1979; Hintze, 1988); salt dissolution (Doelling, 1988; Oviatt, 1988); salt movement (Doelling, 1988). Note that some authors disagree about the period of Moab fault activity.

structures occur at a background density. Near the Delicate Arch Trail, in Arches, this background density is one deformation band every 2 m and one joint every 20 m, whereas in Courthouse Canyon the background density is less than one deformation band or joint every 5 m.

Deformation bands are characterized by positive relief, lighter color relative to the parent rock and a lack of adjacent discontinuity. Their traces are wavy, often anastomosing with surrounding bands. Slip surfaces associated with deformation bands are highly polished with an adjacent ~1-mm-thick zone of highly crushed rock. They occur next to well-developed zones of deformation bands. Deformation bands are 0.5–2 mm thick with large lateral continuity extending hundreds of meters (Aydin and Johnson, 1978; Antonellini and Aydin, 1994; Fossen and Hesthammer, 1997). To calculate the contribution to offset by each deformation band set, we counted the frequency and orientations of deformation bands and assigned a uniform slip value to each deformation band. Representative values of individual deformation band offsets in Fig. 6 were derived from measurements from this paper and data from the literature (Antonellini and Aydin, 1994; Fossen and Hesthammer, 1997). We adopted this method because it is often difficult and time consuming to measure offset across each individual band associated with a larger fault and the distribution of offset values from many field examples fall into a narrow range.

The cross-section trace of joints tends to be straight and is prone to being weathered to negative relief (Zhao and Johnson, 1992). Sheared joints demonstrate shear offset, may have fault rock, and occasionally retain plumose markings. In some cases calcite veins are fractured and

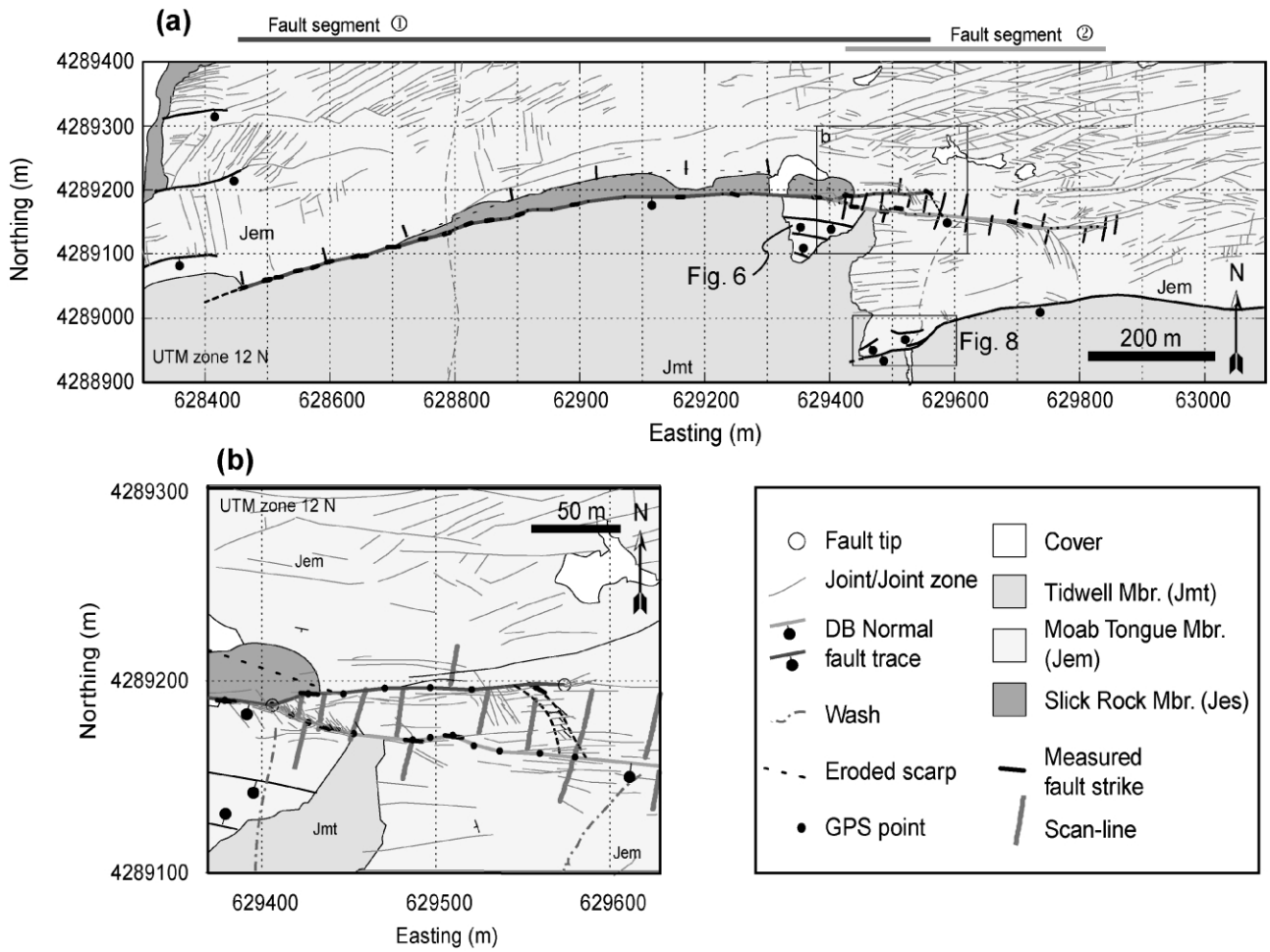

Fig. 5. (a) Tectonic map of the Cache Valley study area (see Fig. 2b for location). Data was collected in two locations: (1) along 29, 20-m-long scan-lines distributed along the length of two linked normal fault segments, and (2) in a detail map and scan-line across small fault segments with only a few meters of offset (boxed areas Fig. 2a). Regional joint sets are spatially restricted to distinct fault-bounded domains. Many joints of short trace length immediately adjacent to the fault are below map resolution. Note that individual deformation bands are not indicated because they are below map resolution. See Antonellini and Aydin (1995) for a detailed deformation band map of part of this area. (b) Detailed map of overlap between fault segments.

reactivated in shear generating cataclasite. Other joints parallel to sheared joints but with no shear provide circumstantial evidence that these structures initially formed as joints. Splay fractures are joints that form at an angle to sheared joints and abut or curve into the trace of the sheared joint. Splay fractures show dominantly opening displacement discontinuity and often manifest plumose structure on the fracture surfaces. Sheared joints and the related splay fractures were recognized in the field by this characteristic angular relationship, abutting geometry, and a sense of offset across the sheared joint (Segall and Pollard, 1983; Cruikshank et al., 1991a,b; Peacock, 2001; Wilkins et al., 2001).

4. Data

We present three examples of fault architecture with an increasing contribution by the sheared joint mechanism. This provides a basis to distinguish how the deformation band-based fault architecture changes as the overprinting joint-based mechanism accommodates greater offset. We use the contrasts between the three examples to examine the relationships of overprinting faulting mechanisms to timing of deformation, the role of pre-existing anisotropy, cumulative offset, and overall fault architecture.

4.1. Case 1: Deformation band faults overprinted by joints: Arches National Park

Both deformation bands and joints (Fig. 7) are prevalent in the Moab Tongue sandstone throughout Cache Valley (Fig. 2b). Faults are primarily composed of deformation bands and zones of deformation bands that form a broad envelope surrounding the fault slip surface (Fig. 8). The density of deformation bands in this envelope decreases away from the fault (Fig. 9). Similarly, joints are spatially

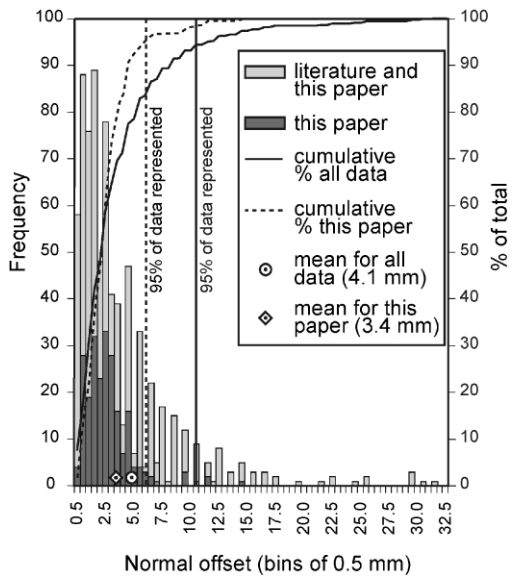

Fig. 6. Measured offset for individual cataclastic deformation bands reported in the literature by Antonellini and Aydin (1994), Fossen and Hesthammer (1997) and this paper in Jurassic sandstones in the Colorado Plateau. These values are used to estimate cumulative offset by deformation bands based on deformation band frequency.

associated with the deformation bands and the associated slip surfaces (Fig. 9).

The distribution of deformation bands and joints around the linked normal fault segments in Fig. 5 varies with position on the fault (Fig. 10). In general, deformation band and joint density are elevated above background densities within approximately 20 m of the slip surface. The density of deformation bands and joints varies along fault strike, but is greatest in the overlap between fault segments 1 and 2 (Fig. 10). Joint density also increases significantly in the tip region while deformation band density increases to a lesser degree in the footwall only (Fig. 10). There is little variation of deformation band density between the footwall and hanging wall of Fault 2.

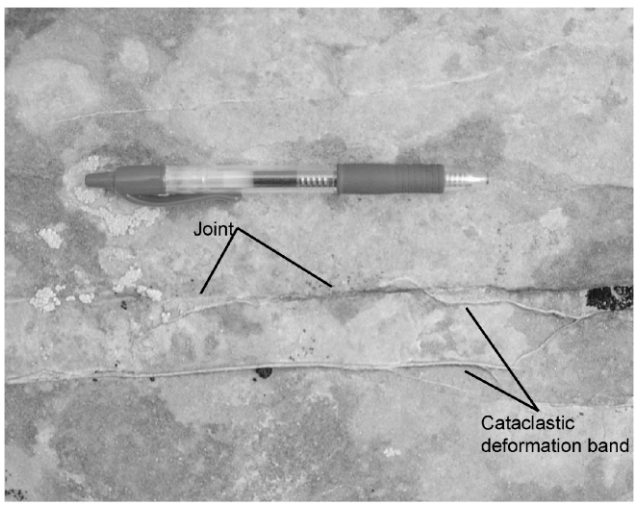

Fig. 7. Detailed photograph of a joint cutting a deformation band.

Throughout the area, joint orientations are affected by proximity to faults on scales ranging from 1 m (Fig. 8) to more than 100 m (Fig. 5). Domains of different joint strike are bounded by faults or related to changes in fault geometry including overlaps between fault segments and fault tips (Fig. 5). In detail joints form in two sets relative to a local fault. The first set is parallel to individual faults, and the strike of the second set forms at an angle to the fault of about 60° (Fig. 8). The first set is distributed adjacent to and along the entire length of the fault and also projects beyond the fault tip (Fig. 11). This set of joints has higher density close to the fault than distant from the fault.

The second set of joints is spatially associated with fault tips (eastern tip of Fault 2 in Fig. 5) and overlaps (Fig. 5b). Within the overlap of faults designated 1 and 2 (Fig. 5b) joints strike obliquely to the fault. These joints are closely spaced at about 50 cm or less with decreasing density away from the intersection of fault segment 2 with fault segment 1. Many of these joints curve to join the fault surface, indicating that they are mechanically interacting with the fault surface (Olson and Pollard, 1981; Cruikshank et al., 1991a,b). Outside the overlap, joints remain parallel to the fault surface with an elevated density within a few meters of the fault slip surface. Joints near several fault tips are oriented at about a 30° angle to the strike of the fault (Figs. 5, 8, 10 and 11). In all cases these joints abut the fault plane and extend into the hanging wall (e.g. Fig. 8). In contrast, deformation bands retain consistent orientations roughly sub-parallel to the fault regardless of position (Fig. 11).

Joints of all orientations consistently cut deformation bands. In addition, the regional set of joints far from faults dip nearly vertical, whereas joints along deformation bands or near faults generally dip 55–80°. These observations indicate that joints are younger than deformation bands and the joints mechanically interacted with pre-existing deformation bands and slip surfaces (Rawnsley et al., 1992; Zhao and Johnson, 1992; Bourne and Willemse, 2001; Peacock, 2001). Fragmented (or very heavily jointed rock) rock is only present in the relay between fault segments 1 and 2. In addition, overlaps between closely spaced en échelon or parallel joints are generally not linked by bridging fractures formed as splay fractures from slip on the original joint. Fragmentation along the eastern margin of the block bounded between the two faults suggests offset on joints in this location, but markers are poor, and millimeter scale offsets may be undetectable in outcrop observation.

The cumulative vertical offset by individual deformation bands along the scan-line in Fig. 8 is 6 m or 18% of the total offset across the faults (Fig. 9). 4.8 and 22.6 m of offset are accommodated across respective slip surfaces along the scan-line. Along fault segments 1 and 2 in Fig. 5 the total offset contributed by individual deformation bands in the damage zone is nearly 7 m of throw, or approximately 15.5% of the total offset across the fault. A lack of breccia due to fragmentation is consistent with the majority of fault

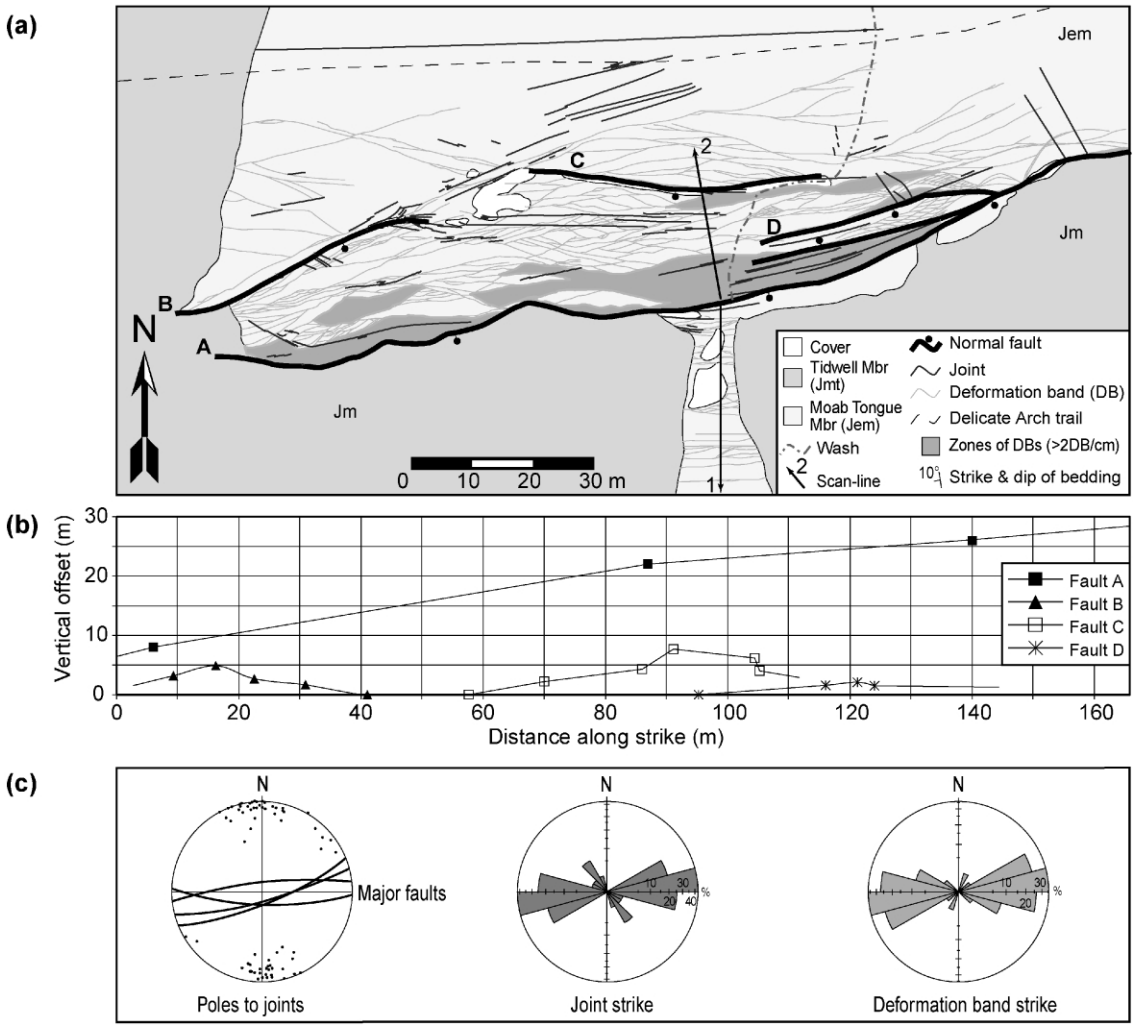

Fig. 8. Detailed map of small faults. (a) Joints, deformation bands, zones of deformation bands, and fault slip surfaces are plotted. (b) Slip distribution across four fault segments in the map labeled A–D. These measurements only represent the offset across the fault surfaces and do not include the contribution to slip by structures in the surrounding damage zone. (c) Comparison of orientations between slip surfaces, joints, and deformation bands.

development and offset during an early phase of faulting by deformation band formation (Fig. 1).

It may be possible to estimate a potential contribution to the offset from the opening of joints associated with this shearing. Joint density is greatest in the overlap region of fault segments 1 and 2 where horizontal offset, or heave, is about 16 m. If joints open s.5 mm (Matthäi et al., 1998) the potential contribution to heave accounting for their orientation relative to the fault is less than 2.5 cm or less than 1% of the heave across the fault surface. This indicates that the development of joints on reactivated faults can result from very small additional offset.

The occurrence of two deformation mechanisms with a consistent age relationship indicates two phases of fault development. The first phase is characterized by the formation of deformation bands with associated slip surfaces. The second phase is characterized by continued slip on fault slip surfaces but additional deformation in the fault and damage zones is accommodated by forming joints. In the case presented above, the contribution by jointing and shearing of joints is only slightly developed. The next section describes an example in which the sheared joint mechanism plays a more important role.

4.2. Case 2: Small offset deformation band fault overprinted by joints and sheared joints: Courthouse Canyon

Multiple cross-sections of seven normal faults are exposed in the walls of Courthouse and Mill Canyons (Fig. 12). The faults are 100–1000 m long with vertical offset between 3 cm and 12 m. Fault surfaces are slickenlined; north dipping faults have rakes between 72° from the east and 88° from the west while south-dipping faults have rakes between 58° from the east and 89° from the west.

The fault in Fig. 13 in Slick Rock sandstone (see Fig. 12 for location) is composed of two elementary structures.

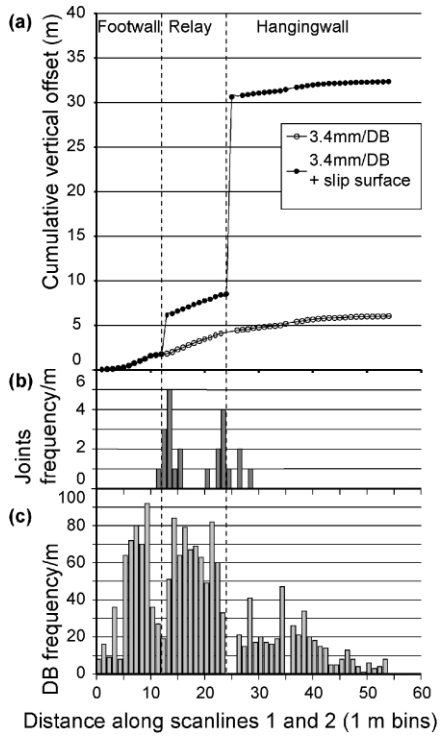

Fig. 9. Scan-line of (a) cumulative vertical offset, (b) joint frequency, and (c) deformation band frequency. Scan-line location is marked in Fig. 8a. Joints are spatially associated with the slip surface. The average deformation band offset taken from measurement of single deformation bands is 3.4 ± 0.8 mm (see Fig. 6).

First, deformation bands are located along all the fault surfaces that accommodate the majority of offset. They are also distributed in zones and single strands around the fault zone. The greatest offset is across a slip surface adjacent to a deformation band zone. Second, joints are spatially associated with and strike parallel to deformation band zones (Fig. 14a and b). They dip primarily either parallel to or abutting against faults at an angle between 15 and 35° to the fault. Examples of each set lack shear offset and have plumose markings on their surfaces indicating they formed as joints (Pollard and Aydin, 1988). We infer that other fractures with similar orientation and morphology also formed as joints.

Joints near faults commonly occur along both individual deformation bands and zones of deformation bands. Since deformation bands dip from 55 to 90°, many of the joints adjacent to deformation bands are inclined to the lithostatic load and are susceptible to normal slip. Antonellini and Aydin (1995) mapped a similar relationship in Arches where the joints also demonstrated shear offset and have splay fractures. In contrast, joints isolated from faults form two near vertical, orthogonal sets striking north–south defining the canyon walls, and east–west. Along all faults, all sets of joints consistently cut deformation bands (e.g. Fig. 13b) indicating that joints are younger. This sequence of development is consistent with the relative timing in the

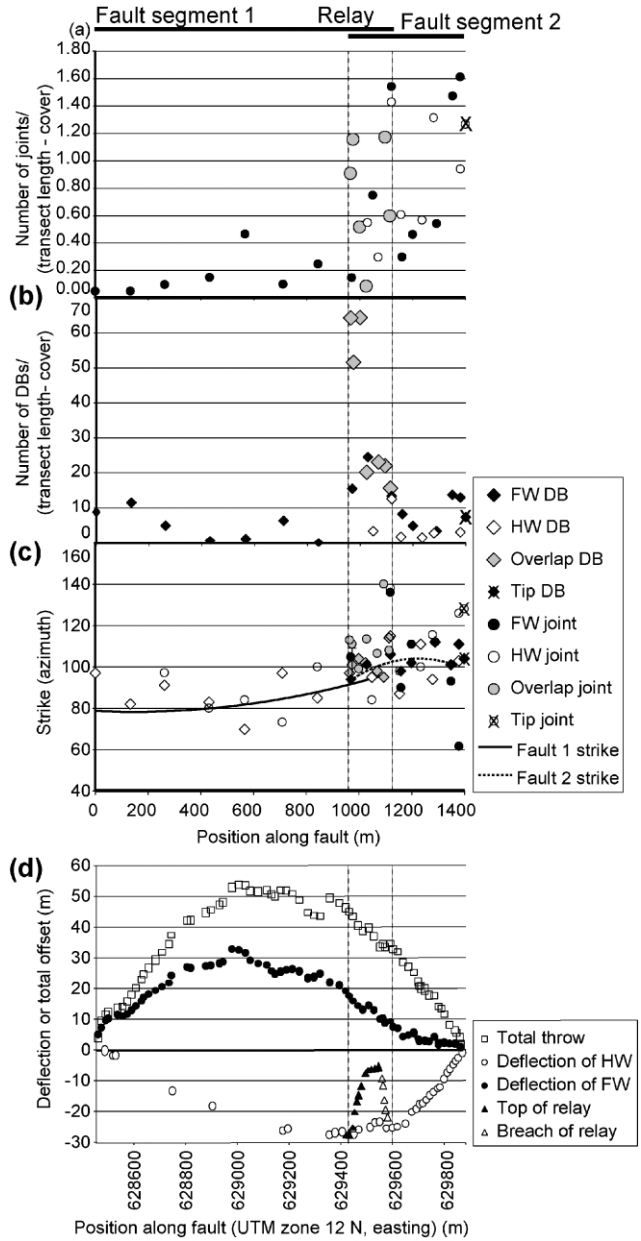

Fig. 10. Mean structure orientation and frequency along strike of fault segments 1 and 2 (Fig. 5a). (a) Variation of joint density expressed as the number of joints along a scan-line divided by the uncovered length of the scan-line. Joint densities are highest in the overlap and near the fault tip. (b) Variation of deformation band density expressed as the number of deformation bands along a scan-line divided by the uncovered length of the scan-line. Deformation band density is highest in the relay. (c) Variation of strike along the fault for deformation bands and joints. Fault strike is interpolated between observation points. The widest range in orientation occurs in the relay and at the eastern fault tip. There is no consistent difference between footwall and hanging wall orientations. Away from geometric complexity both joints and deformation bands parallel the orientation of the fault. (d) Offset along fault segments 1 and 2. Hanging wall and footwall deflection are similar orders of magnitude. A 4° regional dip has been removed from the data to emphasize the offset distribution. The relay is fully breached; the total offset gradient is not affected by its presence.

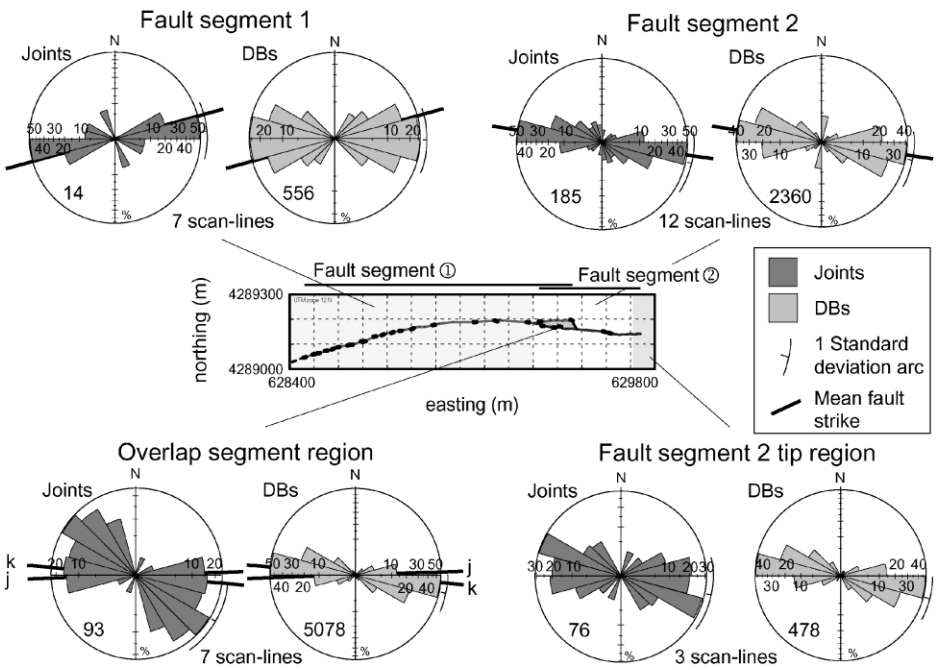

Fig. 11. Rose diagrams of joints and deformation bands for different structural positions along the two overlapping faults.

Salt Valley and Cache Valley areas proposed by earlier workers (Cruikshank et al, 1991a,b; Antonellini and Aydin, 1995).

Many joints abut sheared joints and fault slip surfaces at an angle between 15 and 50° (Fig. 13). These joints typically have no shear offset and occasionally have plumose markings indicating they are opening mode structures. The line of intersection of splay joints with the sheared joint should be normal to the slip direction (Martel and Boger, 1998; Wilkins et al., 2001). These joints are consistent in geometry, slip direction measured from slickenlines and sense of offset on the sheared joint with the formation of splay fractures (Fig. 14c). Offset across a sheared joint leading to splay fracture formation is generally between 1 mm and 1 cm. This geometry provides a further basis for identifying sheared joints.

The density of deformation bands, joints and sheared joints increase near the fault (Figs. 13 and 15). The increase in sheared joint density is associated with an increasing frequency of splay fractures accompanying greater slip on sheared joints near the fault (Fig. 13b). Discontinuous pockets of breccia form in geometric complexities like overlaps between en échelon slipping joints, at bends in a slip surface, or at intersections between a slipping surface and sedimentary layering. The overprinting of joints along deformation bands away from the fault surface indicates that the presence of the older deformation bands has affected the distribution of damage due to jointing.

The fault geometry resembles a conjugate fault pattern defined by two sets of normal faults striking parallel but dipping in opposite directions (Fig. 13). This pattern develops sequentially as new joints form as splay fractures generated from older joints (Davatzes and Aydin, 2003) or deformation band slip surfaces reactivated in shear.

Sheared joints, splay fractures and fragmentation zones and breccia indicate that additional offset occurred across the fault surface following the cessation of the deformation band mechanism. The primary fault surface in Fig. 13 accommodates 2.3 m of vertical offset. If each splay fracture across the fault contributes 1 mm of opening and represents the corresponding offset by the second phase of deformation, then the total offset due to this phase is about 60 cm or 26% of the slip on the reactivated deformation band slip surface (Fig. 15d). This is consistent with reports by Myers (1999), Cruikshank and Aydin (1994) and Davatzes and Aydin (2003) for the onset of fragmentation leading to breccia formation (Fig. 1). The total offset across the fault zone including its damage zone is 3.8 m, 1.5 m of which is distributed through the damage zone. This indicates that damage accrues rapidly in the vicinity of the fault even at small offsets.

4.3. Case 3: Large offset normal fault with significant abundance of overprinting joint-based faulting structural elements: Courthouse Canyon

The distribution of structures along a scan-line across the Moab fault was measured in the Slick Rock Member of the Entrada Formation along a wall of the Courthouse Canyon (Fig. 12). The scan-line is 86 m long and projects 70 m into the footwall from the hanging wall side of the fault zone.

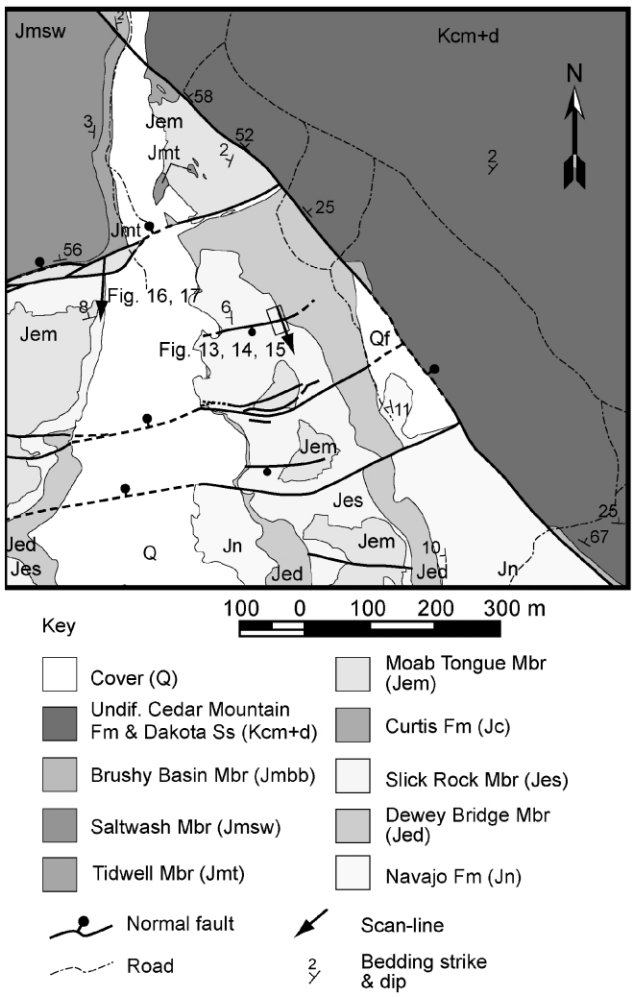

Fig. 12. Tectonic map of Courthouse Canyon area along the Moab fault. The location of the scan-line across the Moab fault segment in Fig. 16, and the detailed map and scan-line across the small fault in Figs. 13–15 are indicated. Courthouse Rock is located at 38°42′35″N, 109°42′44″W.

The total vertical offset across the Moab fault in this location is 110 m.

The fault zone in this location is approximately 15 m wide and is defined by two slip surfaces related to a zone of deformation bands along either slip surface. The slip surface on the hanging wall side drops Moab Tongue sandstone more than 25 m. Each slip surface is bordered by a well-defined zone of deformation bands a few meters thick. Fault rock includes fracture bounded rock fragments with slickensided surfaces and deformation band zones in Slick Rock and Moab Tongue sandstone. One meter of shaley fault gouge derived from the Morrison Formation has developed along the slip surface on the hanging wall side of the fault zone. Units in the Morrison Formation in the hanging wall strike roughly parallel to the fault zone; dip decreases from a maximum value of 67° adjacent to the fault zone to the regional dip 100 m from the fault.

Damage in the footwall extends for 51 m from the fault zone before the frequency of component structures reaches

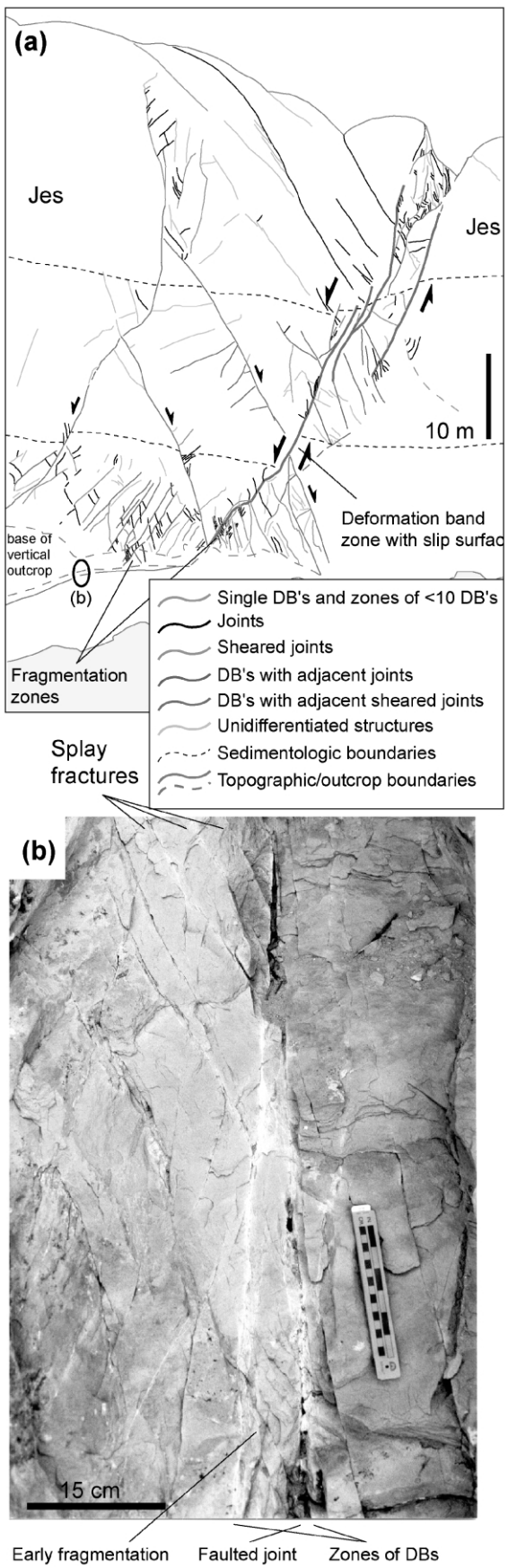

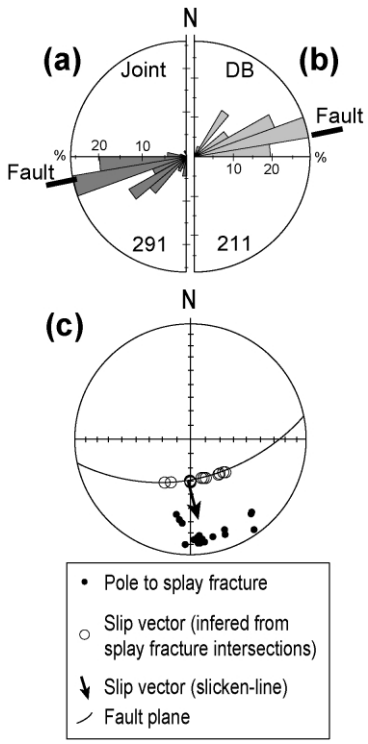

Fig. 14. Orientation data for fault in Fig. 13. (a) Rose diagram of joint and sheared joint orientations. (b) Rose diagram of deformation band orientations. (c) Fault plane and slip vector from slickenlines compared with slip vectors predicted from first generation splay fractures.

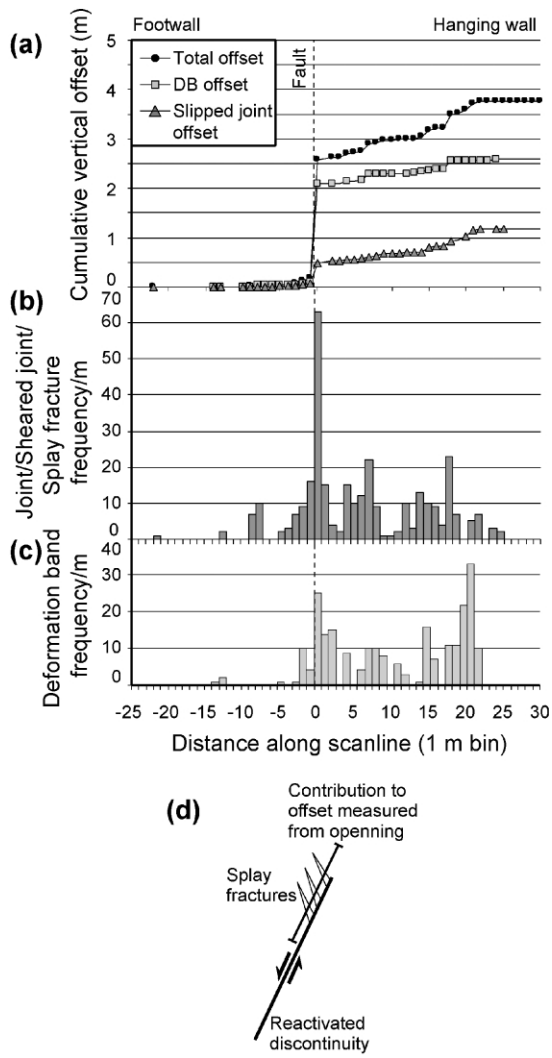

Fig. 15. Scan-line data from small faults in Courthouse Canyon area. (a) Cumulative vertical offset from deformation bands, joints and sheared joints, and the main slip surface of the fault in Fig. 13 using the average offset per deformation band from Fig. 6. (b) Frequency of joints and sheared joints. (c) Frequency of deformation bands. (d) Graphical representation of contribution to offset by opening of splay fractures.

the background density. Small faults are located at irregular intervals for another 500 m but with well-defined gaps at the background density of structures. Within the damage zone, the densities of both joints and deformation bands decreases with increasing distance from the fault (Fig. 16) similar to other examples in this paper. Joints and sheared joints are equally prominent in the fault zone and adjacent to the fault zone in the footwall. This results because many splay fractures were reactivated in shear and produced their own splay fractures. The process of reactivating splay fractures is most prominent in the fault zone and adjacent to the bounding slip surfaces in the damage zone.

Both deformation mechanisms make a significant contribution to offset across the combined Moab fault zone and its damage zone (Fig. 17) in this location. The total vertical offset due to: (1) slip on reactivated joints is 30.10 m (21.1% of the total); (2) individual deformation bands is 6.53 m (4.6% of the total), and (3) fault zone-bounding deformation band slip surfaces active during both phases of faulting is 106 m (74.4% of the total). Reactivation of slip surfaces during a joint-dominated deformation phase is postulated from the development of breccia along these surfaces consistent with splay fracture formation and the accompanying high density of splay fractures in the fault zone. A minimum extension due to joint formation and veining is recorded by 66 cm of vein thickness within the fault and damage zone (Fig. 16d). The consistent observation that joints are younger than deformation bands supports a distinct transition in faulting mechanism from entirely deformation banding to jointing at any single location. This is the same relationship observed in other locations (see Figs. 13 and 15).

Within the damage zone, all structural components strike sub-parallel to the fault zone and most of them dip in the same direction. In contrast, between the two bounding slip

Fig. 13. Joints, sheared joints and deformation bands in Courthouse Rock. (a) Detailed map of structures constituting a small fault in the east face of Courthouse Rock (Fig. 12). (b) Faulted joint with splay fractures overprinting older deformation band structures located in (a). Between two sheared joints, high splay fracture density fragments the rock.

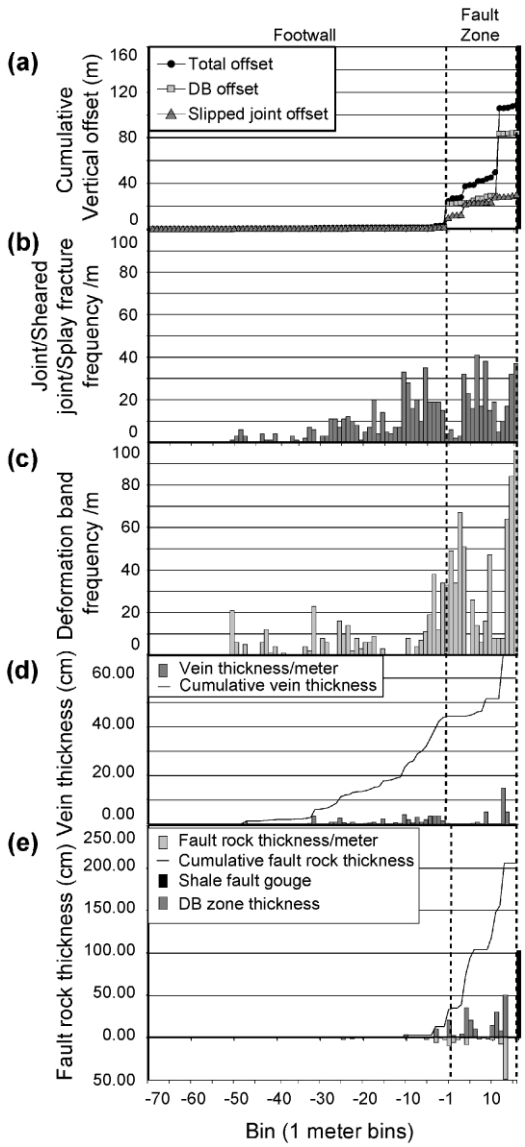

Fig. 16. Scan-line data from fault and damage zone of Moab fault segment in Courthouse Canyon. (a) Cumulative offset across the fault zone from different deformation mechanisms. The cumulative offset contributed by individual deformation bands is estimated using the average offset per deformation band from Fig. 6. The total offset is approximately 110 m. (b) Frequency of all structures formed initially as joints including, joints, sheared joints and splay fractures per meter. (c) Deformation band frequency per meter. (d) Vein thickness as a function of distance from the fault. (e) Fault rock thickness as a function of distance from the fault. There are two types of fault rock in the sandstone. (1) Breccia and fault rock principally resulting from splay fracture fragmentation of the rock. Areas of fault rock are bordered by high densities of splay fractures. (2) Deformation bands and zones of deformation bands. Nearly all fault rock is located in the fault zone.

surfaces that define the fault zone, there is no consistent orientation of structures; both deformation bands and joints have a wide range of strike and dip. The rake on slip surfaces bounding the fault zone ranges from 78 to 88° from the east. In contrast, rakes on slickensided surfaces within the fault zone show greater variation and range from 56° from the east to 86° from the west.

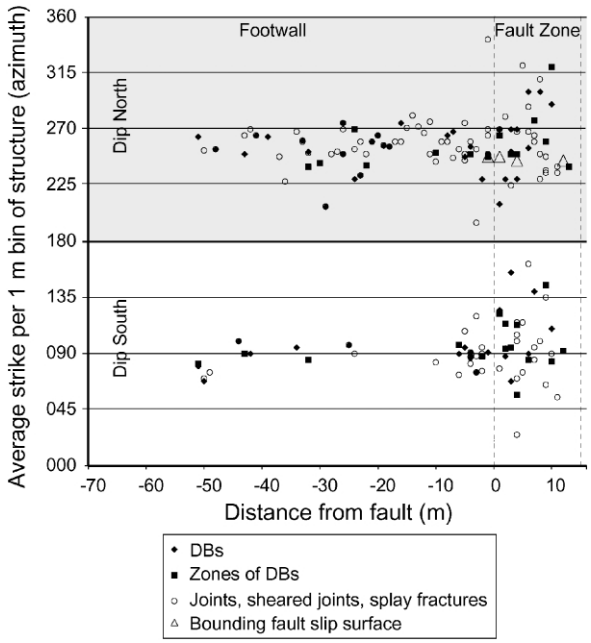

Fig. 17. Orientations of structures along scan-line across Moab fault in Courthouse Canyon. Structures measured within the damage zone strike within a small range, whereas the orientation of structures within the fault zone are highly variable.

5. Discussion

5.1. Architecture and partitioning of deformation mechanisms and their contributions

The two end-member deformation mechanisms outlined in Fig. 1 generate faults with distinct fault architectures as slip increases. We contend that the distribution and number of different structures composing a fault depend on the relative contributions of overprinting mechanisms to the total offset, and on their relative timing. The contribution to offset by a particular deformation mechanism indicates the portion of fault development by this mechanism. The distribution, orientation, offset, and type of structures are related to the relative contribution of each mechanism to the total offset.

Fault rocks developed by each system are different in distribution and continuity. Deformation band zones and highly comminuted zones adjacent to the slip surfaces demonstrate large lateral extents and continuity. In contrast, breccia and fault rock associated with shearing along joints may be discontinuous depending on the initial geometry (Myers, 1999; Taylor et al., 1999) of discontinuities localizing shear and the magnitude of offset. Joints form preferentially at fault overlaps and tips leading to a spatial variation in joint density both along strike (Figs. 5 and 7) and in cross-section (Fig. 13). In contrast, deformation band densities are elevated in overlaps but form at a fairly consistent density along the fault and beyond the fault tip (Fig. 11). Overprinting of these two mechanisms in the same rock at a single location produces

composite fault architecture. Furthermore, spatially or temporally varying conditions may lead to a heterogeneous distribution of the structural elements associated with the sheared joint faulting mechanism. The parameters, such as variation in material properties and/or in the stress state, that control the distribution of component structures along a developing fault zone are important subjects for future work.

The progression of examples from simple cases with only a small contribution by joint development in Arches to cases where each deformation mechanism accommodates a significant proportion of the slip along the Moab fault demonstrates increasing variation (heterogeneity) in the density of component structures in the fault zones. In the Courthouse Canyon, the contribution from joint formation is manifested by the magnitude of slip accommodated by shearing of joints, the joint density and the formation of breccia. The overprinting of these faults by a second mechanism introduces extensive, localized, heterogeneity in the distribution of structural components (e.g. Fig. 13) along even a very simple fault. One key parameter determining the final composition of the fault architecture is the relative contribution of each deformation mechanism to offset and the relative timing of the mechanisms.

Faults examined in Arches versus along the Moab fault scan-line have comparable deformation band densities despite the very different magnitudes of total offset. All three cases have well-defined damage zones with a high density of structural elements. The density of these structural elements approaches a background value away from the faults. The similar deformation band densities in faults with very different dimensions and offset may suggest that much of the cataclastic deformation in these zones is inherited from an early stage of faulting, perhaps from fault nucleation or propagation. High deformation band and joint density (Fig. 10a and b) ahead of fault tips and in overlaps are also qualitatively consistent with the role of fault propagation in producing a damage zone around a fault. In contrast, the overprinting of a second faulting mechanism clearly indicates that the faults accrued a significant proportion of additional damage during the joint-based faulting. For instance, the examples from the Moab fault indicate that a large proportion of the total slip was accommodated by the joint-based mechanism (Figs. 15 and 16). Because of the overprinting relationship, we can deduce that the joint-based portion of the deformation occurred after fault nucleation and development of the general fault geometry. These observations indicate that the deformation mechanisms and slip history may play key roles in determining how damage is distributed around faults at different stages of their development.

5.2. Interaction of overprinting deformation mechanism with products of an earlier mechanism

Cataclastic deformation bands composing the Moab fault demonstrate porosity loss and grain crushing that produces volume loss in the band. Mair et al. (2000) has produced similar deformation bands in the laboratory, characterized by grain crushing, volume loss and the formation of multiple adjacent bands, under a single, consistent compressive stress state. However, further experiments are required to determine the potential range of stress states in which cataclastic deformation bands may form. In contrast, joints demonstrate opening displacement discontinuity and thus dilation. The formation of joints requires local tensile stresses greater than the tensile strength of the rock being deformed (Pollard and Aydin, 1988). Subsequent shearing of these discontinuities results from the resolution of shear stresses on the joint surfaces greater than the product of the coefficient of friction and the normal stress acting on that surface. The occurrence of both structures along a single fault could be accounted for by a change of stress state from compressive stresses to at least locally effective tensile stresses. Consequently, the change from compactive shear failure to opening mode failure may require distinct deformation mechanisms contributing to fault development associated with distinct deformation conditions.

Deformation bands and their related slip surfaces represent a mechanical anisotropy that is exploited by subsequent joint formation. Slip surfaces, once established, are inclined, mechanically weak discontinuities susceptible to reactivation in subsequent normal faulting events. Following a change in deformation environment, such as a reduction in confining stress or increase in fluid pressure, jointing may become a viable deformation mechanism. Slip localized on the previously established slip surface during this period will promote the formation of splay fractures. If slip continues, splay fracture density will increase leading to breccia formation and a significant change in the architecture of the fault and damage zone.

A causative relationship between fault dimensions, fault zone width, and total offset (e.g. Evans, 1990; Scholz et al., 1993; Foxford et al., 1998; Beach et al., 1999; Fossen and Hesthammer, 1997; Shipton and Cowie, 2001) implicitly presupposes continuous fault zone development and fault propagation by a single mechanism or that these requirements are inconsequential. Pre-existing structures are a key element of splay fracture formation; propagation of a fault by this mechanism involves the linking of other pre-existing structures by splay fracture formation (Segall and Pollard, 1983; Myers, 1999; Flodin, 2003). Wilkins et al. (2001) demonstrate that the dimensions of pre-existing joints that subsequently localize slip have a significant impact on the scaling relationship between fault dimensions and slip magnitude. In the same manner, this paper emphasizes the role of distinct mechanisms in determining the statistical characteristics of faults.

Aydin and Johnson (1978) suggest that porosity reduction accompanying deformation band formation causes an increase in the stiffness of the band. A deformation band therefore acts as a stiff inclusion in a

less stiff matrix in a manner formulated by Eshelby (1957). This stiffness contrast may concentrate stress around the previously formed deformation bands leading to the preferred formation of joints along pre-existing deformation bands. The ability of deformation bands to concentrate stress and the stress perturbation around a slipping fault may also combine to create a high density of joints near a fault. Finally, the increase in deformation band density near the fault may further increase the magnitude of the stress perturbation by increasing the width of the stiff inclusion (Eshelby, 1957; Engelder, 2000). However, the fact that there are deformation band faults without joints is evidence for a more substantial change either in the stress state or in the constitutive behavior of sandstones being responsible for the shift from one deformation mechanism to the other.

5.3. Implications for fluid flow prediction

The gross permeability of a fault including the surrounding damage zone is a product of the permeability of individual structures and their geometry (Caine et al., 1996, 1999; Matthäi et al., 1998; Taylor et al., 1999; Aydin, 2000; Flodin et al., 2001; Jourde et al., 2002). Consequently, models that predict the distribution, orientation, and connectivity of structures composing a fault can be extended to infer the permeability structure of a fault. The cases investigated above show that the architecture of faults changes significantly through time as the deformation mechanism changes and new structures are added. Whereas deformation bands act as fluid barriers (Antonellini and Aydin, 1994), joints and slightly sheared joints and breccia zones act as fluid conduits (Dholakia et al., 1998; Taylor et al., 1999). The process of splay fracturing along sheared joints creates a well-connected network of joints, improving fluid transmission. Joints in the field area are filled with both bitumen and calcite (Foxford et al., 1996).

This implies that the faults were first sealing, but that overprinting by jointing and brecciation may have created a well-connected joint network. As a result, fault parallel fluid flow may be enhanced and cross-fault flow may be possible along crosscutting joints. Therefore the permeability of the faults evolves over time even after significant offset has been established because the types of structures composing a fault zone change. However, a precise evaluation of the impact of overprinting joints on the failure of an existing fault trap depends on the connectivity of joints across sealing fault rock and on either side of the fault rock.

6. Conclusions

Two mechanisms contribute to fault development in sandstone in Cache Valley in Arches National Park and in the Moab-Spanish Valley. These faults are composed of deformation bands and associated slip surfaces overprinted by joints, sheared joints and breccia. We have studied a number of faults in porous sandstones in Cache Valley in the Arches National Park. These faults initially formed by deformation banding and were subsequently overprinted by joints associated with slip on the established faults.

Two examples from the Moab fault system demonstrate overprinting of deformation bands by joints and subsequent shearing of the joints leading to brecciation associated with continued slip on the faults. These structures and their formation sequence indicate that two mechanisms contributed to fault development. A consistent analysis of fault architecture requires partitioning the offset between deformation band and sheared joint-based faulting mechanisms and assessing their relative impact on the nature and distribution of the structural components. Individual structures and their contribution to faulting can be recognized even at large offsets exceeding 100 m. This methodology defines a potential tool for analyzing fault systems based on the occurrence, timing, and distribution of deformation mechanisms and the associated structures as a means to assess fault history and sealing potential through time.

The distribution and orientation of deformation bands and joints are both sensitive to position on the fault. The presence and arrangement of early deformation bands significantly affects the distribution of both joints and sheared joints. Breccia and fault rock accompanying shearing along joints compared with deformation bands and highly comminuted slip surfaces, are different in distribution and continuity. Overprinting of the two faulting mechanisms in the same rock in a single location produces heterogeneous, composite fault architectures. Slip surfaces and deformation bands demonstrate large lateral extent, whereas breccias are typically discontinuous depending on the initial joint geometry and magnitude of offset. Identifying and mapping variation of these controlling parameters provides a basis for predicting fault zone heterogeneity and understanding the process of fault growth. These results are highly critical for assessing fault zone permeability and fault seal potential in clastic reservoirs because initially sealing faults may be breached by cross-cutting joints during a second stage of faulting.

Acknowledgements

This work greatly benefited from support and contributions by Peter Eichhubl who helped in the field and reviewed the manuscript. Stephan Bergbauer provided valuable help, making one of the field sessions devoted to this project productive. Marco Antonellini provided valuable remarks on the manuscript and Mary Beth Gray helped with the clarity of the manuscript. I would also like to acknowledge the help, environment and financial support provided by the Rock Fracture Project that contributed to

the completion and quality of this work. Finally, we would like to thank Dr Conrad Childs, Dr Sarah Tindall, and the editor Dr Jim Evans for constructive reviews of the manuscript.

References

Antonellini, M., Aydin, A., 1994. Effect of faulting on fluid flow in porous sandstones: petrophysical properties. American Association of Petroleum Geologists Bulletin 78 (3), 355–377.

Antonellini, M., Aydin, A., 1995. Effect of faulting on fluid flow in porous sandstones: geometry and spatial distribution. American Association of Petroleum Geologists Bulletin 79 (5), 642–671.

Antonellini, M.A., Aydin, A., Pollard, D.D., 1994. Microstructure of deformation bands in porous sandstones at Arches National Park, Utah. Journal of Structural Geology 16 (7), 941–959.

Aydin, A., 2000. Fractures, faults, and hydrocarbon entrapment, migration and flow. Marine and Petroleum Geology 17, 797–814.

Aydin, A., Johnson, A.M., 1978. Development of faults as zones of deformation bands and as slip surfaces in sandstone. Pure and Applied Geophysics 116, 931–942.

Barton, C.C., 1983. Systematic jointing in the Cardium Sandstone along the Bow River, Alberta, Canada. Ph.D. dissertation. Yale University, Connecticut, 337pp.

Beach, A., Welbon, A.L., Brockbank, P., McCallum, J.E., 1999. Reservoir damage around faults: outcrop examples from the Suz rift. Petroleum Geoscience 5, 109–116.

Bourne, S.J., Willemse, E.J.M., 2001. Elastic stress control on the pattern of tensile fracturing around a small fault network at Nash Point, UK. Journal of Structural Geology 23, 1753–1770.

Brace, W.F., Bombolakis, E.G., 1963. A note on brittle crack growth in compression. Journal of Geophysical Research 68 (12), 3709–3713.

Caine, J.S., Evans, J.P., Forster, C.B., 1996. Fault zone architecture and permeability structure. Geology 24 (11), 1025–1028.

Caine, J.S., Evans, J.P., Forster, C.B., 1999. Fault zone architecture and fluid flow: insights from field data and numerical modeling. In: Haneberg, W.C., Mozley, P.S., Moore, J.C., Goodwin, L.B. (Eds.), Faults and Subsurface Fluid Flow in the Shallow Crust. Geophysical Monograph 113, pp. 101–127.

Cater, F.W., 1970. Geology of the salt anticline region in southwestern Colorado, with a section on stratigraphy by Fred W. Cater and Lawrence C. Craig. United States Geological Survey Professional Paper P0637, 80pp.

Chan, M.A., Parry, W.T., Bowman, J.R., 2000. Diagenetic hematite and manganese oxides and fault-related fluid flow in Jurassic sandstones, southeastern Utah. American Association of Petroleum Geologists Bulletin 84 (9), 1281–1310.

Chan, M.A., Parry, W.T., Petersen, E.U., Hall, C.M., 2001. $^{40}Ar/^{39}Ar$ age and chemistry of manganese mineralization in the Moab and Lisbon fault systems, southeastern Utah. Geology 29 (4), 331–334.

Cooke, M.L., 1997. Fracture localization along faults with spatially varying friction. Journal of Geophysical Research 102 (10), 22,425–22,434.

Cruikshank, K.M., Aydin, A., 1994. Role of fracture localization in arch formation, Arches National Park, Utah. Geological Society of America Bulletin 106 (7), 879–891.

Cruikshank, K.M., Zhao, G., Johnson, A.M., 1991a. Analysis of minor fractures associated with joints and faulted joints. Journal of Structural Geology 13 (8), 865–886.

Cruikshank, K.M., Zhao, G., Johnson, A.M., 1991b. Duplex structures connecting fault segments in Entrada Sandstone. Journal of Structural Geology 13 (10), 1185–1196.

Davatzes, N.C., Aydin, A., 2003. Overprinting faulting mechanisms during the development of multiple fault sets in sandstone, Chimney Rock fault array, Utah. Tectonophysics 363, 1–18

Davatzes, N.C., Aydin, A., 2003. Formation of conjugate fault systems in folded sandstone. Journal of Geophysical Research.

Davis, G.H., 1999. Structural geology of the Colorado Plateau regional of southern Utah, with special emphasis on deformation bands. Geological Society of America (GSA), Boulder, CO, Special Paper 342, 157pp.

Dholakia, S.K., Aydin, A., Pollard, D.D., Zoback, M.D., 1998. Fault-controlled hydrocarbon pathways in the Monterey Formation, California. American Association of Petroleum Geologists Bulletin 82 (8), 1551–1574.

Doelling, H.H., 1985. Geology of Arches National Park. Utah Geological and Mineral Survey, Salt Lake City, UT.

Doelling, H.H., 1988. Geology of Salt Valley Anticline and Arches National Park, Grand County, Utah. Salt deformation in the Paradox region. In: Doelling, H.H., Oviatt, C.G., Huntoon, P.W. (Eds.), Salt Deformation in the Paradox Region. Utah Geological and Mineral Survey, Salt Lake City, UT. Bulletin 122, pp. 1–60.

Doelling, H.H., 1996. Geologic map of the Dewey Quadrangle, Grand County, Utah. Utah Geological and Mineral Survey, Salt Lake City, UT.

Dyer, J.R., 1983. Jointing in sandstones, Arches National Park, Utah. Ph.D. thesis, Department of Geology, Stanford University, Stanford, California.

Engelder, J.T., 1974. Cataclasis and the generation of fault gouge. Geological Society of America Bulletin 85 (10), 1515–1522.

Engelder, J.T., 1987. Joints and shear fractures in rock. In: Atkinson, B.K. (Ed.), Fracture Mechanics of Rock. Academic Press, London, UK, pp. 27–69

Engelder, J.T., 2000. Joint interaction with embedded concretions: joint loading configurations inferred from propagation paths. Journal of Structural Geology 21 (8–9), 1049–1055.

Eshelby, J.D., 1957. The determination of the elastic field of an ellipsoidal inclusion, and related problems. Proceedings of the Royal Society of London 241a, 376–396.

Evans, J.P., 1990. Thickness–displacement relationships for fault zones. Journal of Structural Geology 12, 1061–1065.

Fletcher, R.C., Pollard, D.D., 1981. Anticrack model for pressure solution surfaces. Geology 9 (9), 419–424.

Flodin, E.A., 2003. Structural evolution, petrophysics, and large-scale permeability of faults in sandstone, Valley of Fire, Nevada. Ph.D. dissertation. Stanford University, California, 180pp.

Flodin, E.A., Aydin, A., Durlofsky, L.J., Yeten, B., 2001. Representation of fault zone permeability in reservoir flow models. SPE paper 71671. SPE Annual Technical Conference and Exhibition, New Orleans, p. 10.

Fossen, H., Hesthammer, J., 1997. Geometric analysis and scaling relations of deformation bands in porous sandstone. Journal of Structural Geology 19, 1479–1493.

Foxford, K.A., Garden, S.C., Guscott, S.D., Burley, S.D., Lewis, J.J.M., Walsh, J.J., Watterson, J., 1996. The field geology of the Moab Fault. In: Huffman, A.C.J., Lund, W.R., Godwin, L.H. (Eds.), Geology and Resources of the Paradox Basin 25. Utah Geological Association Guidebook, pp. 265–283.

Foxford, K.A., Walsh, J.J., Watterson, J., Garden, I.R., Guscott, S.C., Burley, S.D., 1998. Structure and content of the Moab Fault zone, Utah, USA, and its implications for fault seal prediction. In: Jones, G.A.K., Fisher, Q.J., Knipe, R.J. (Eds.), Faulting, Fault Sealing and Fluid Flow in Hydrocarbon Reservoirs, Special Publications 147, Geological Society, London, pp. 87–103.

Friedman, J.D., Case, J.E., Simpson, S.L., Heller, J.S., 1994. Tectonic trends of the northern part of the Paradox Basin, southeastern Utah and southwestern Colorado, as derived from Landsat multispectral scanner imaging and geophysical and geologic mapping. Uncontrolled X-band radar mosaic of the western part of the Moab $1° \times 2°$ Quadrangle, southeastern Utah and southwestern Colorado. U.S. Geological Survey, Reston, VA.

Garden, I.R., Guscott, S.C., Foxford, K.A., Burley, S.D., Walsh, J.J., Watterson, J., 1997. Iron oxide reduction as evidence for hydrocarbon migration through the Entrada Sandstone of the Moab Anticline, Utah. In: American Association of Petroleum Geologists 1997 Annual

Convention. Annual Meeting Abstracts—American Association of Petroleum Geologists and Society of Economic Paleontologists and Mineralogists 6. Tulsa, OK: American Association of Petroleum Geologists and Society of Economic Paleontologists and Mineralogists, 1997, Dallas, TX, p. 45.

Garden, I.R., Guscott, S.C., Burley, S.D., Foxford, K.A., Walsh, J.J., Marshall, J., 2001. An exhumed paleo-hydrocarbon migration fairway in the Entrada Sandstone of SE Utah, USA. Geofluids 1 (3), 195–213.

Ge, H., Jackson, M.P.A., Vendeville, B.C., Hudec, M.R., 1994. Initiation and early growth of salt structures in the Paradox Basin, Utah and Colorado; insights from dynamically scaled physical experiments. In: AAPG Annual Convention. Annual Meeting Abstracts—American Association of Petroleum Geologists and Society of Economic Paleontologists and Mineralogists 1994. Tulsa, OK: American Association of Petroleum Geologists and Society of Economic Paleontologists and Mineralogists, 1994, Denver, CO, p. 154.

Gentier, S., Riss, J., Archambault, G., Flamand, R., Hopkins, D., 2000. Influence of fracture geometry on shear behavior. International Journal of Rock Mechanics and Mining Sciences 37, 161–174.

Granier, T., 1985. Origin, damping, and pattern of development of faults in granite. Tectonics 4 (7), 721–737.

Hintze, L.F., 1988. Geologic history of Utah. Brigham Young University Geology Studies; Special Publication 7. Brigham Young University, Provo, UT. 202pp.

Hunt, C.B., 1969. Geologic history of the Colorado River. U.S. Geological Survey Professional Paper P0669-C, C59–C130.

Jamison, W.R., Stearns, D.W., 1982. Tectonic deformation of Wingate Sandstone, Colorado National Monument. American Association of Petroleum Geologists Bulletin 66 (12), 2584–2608.

Jourde, H., Flodin, E., Aydin, A., Durlofsky, L.J., Wen, X.H., 2002. Large scale permeability of fault zones in porous sandstone: from detailed field measurements to numerical modeling. American Association of Petroleum Geologists Bulletin 86, 1187–1200.

Knipe, R.J., 1997. Juxtaposition and seal diagrams to help analyze fault seals in hydrocarbon reservoirs. American Association of Petroleum Geologists Bulletin 81 (2), 187–195.

Lin, P., Logan, J.M., 1991. The interaction of two closely spaced cracks: a rock model study. Journal of Geophysical Research 96 (13), 21, 667–21,675.

Lucchitta, I., 1979. Late Cenozoic uplift of the southwestern Colorado Plateau and adjacent lower Colorado River region. In: The Geological Society of America, Rocky Mountain Section, 32nd Annual Meeting 11, no. 6. Boulder, CO: Geological Society of America (GSA), March 1979, Fort Collins, CO, p. 278.

Mair, K., Main, I., Elphick, S., 2000. Sequential growth of deformation bands in the laboratory. Journal of Structural Geology 22 (1), 25–42.

Martel, S.J., 1990. Formation of compound strike-slip fault zones, Mount Abbot Quadrangle, California. Journal of Structural Geology 12 (7), 869–882.

Martel, S.J., Boger, W.A., 1998. Geometry and mechanics of secondary fracturing around small three-dimensional faults in granitic rock. Journal of Geophysical Research 103 (9), 21299–21314.

Martel, S.J., Pollard, D.D., Segall, P., 1988. Development of simple fault zones in granitic rock, Mount Abbot Quadrangle, Sierra Nevada, California. Bulletin of the Geological Society of America 100, 1451–1465.

Matthäi, S.K., Aydin, A., Pollard, D.D., Roberts, S., 1998. Numerical simulation of deviations from radial draw-down in a faulted sandstone reservoir with joints and zones of deformation bands. In: Jones, G., Fisher, Q.J., Knipe, R.J. (Eds.), Faulting, Fault Sealing and Fluid Flow in Hydrocarbon Reservoirs, Special Publication 147, Geological Society, London, pp. 157–191.

Molenaar, C.M., 1987. Mesozoic rocks of Canyonlands country. In: Campbell, J.A. (Ed.), Geology of Cataract Canyon and Vicinity 1987. Field Symposium—Guidebook of Four Corners Geological Society 10, pp. 19–24.

Myers, R.D., 1999. Structure and hydraulic properties of brittle faults in sandstone. Ph.D. dissertation. Stanford University, California, 176pp.

Myers, R.D., 2003. The evolution of faults formed by shearing across joint zones in sandstone. Journal of Structural Geology, submitted.

Nemat-Nasser, S., Horii, H., 1982. Compression-induced non-planar crack extension with application to splitting, exfoliation, and rockburst. Journal of Geophysical Research 87 (8), 6805–6821.

Nuccio, V.F., Condon, S.M., 1996. Burial and thermal history of the Paradox Basin, Utah and Colorado, and petroleum potential of the Middle Pennsylvanian Paradox Basin. U.S. Geological Survey, Reston, VA.

Nuccio, V.F., Condon, S.M., 1999. Burial and thermal history of the Paradox Basin, Utah and Colorado, and petroleum potential of the middle Pennsylvanian Paradox Formation. In: Huffman, A.C.J., Lund, W.R., Godwin, L.H. (Eds.), Geology and Resources of the Paradox Basin. Utah Geological Association Guidebook 25, pp. 57–76.

Ohlmacher, G.C., Aydin, A., 1993. Mechanics of vein, fault and solution surface formation in the Appalachian Valley and Ridge, northeastern Tennessee, USA; implications for fault friction, state of stress and fluid pressure. Journal of Structural Geology 19, 927–944.

Olig, S.S., McCleary, J., Wong, I.G., 1996. The earthquake potential of the Moab Fault and its relation to salt tectonics in the Paradox Basin, Utah. In: Huffman, A.C.J., Lund, W.R., Godwin, L.H. (Eds.), Geology and Resources of the Paradox Basin. Utah Geological Association Guidebook 25, pp. 251–264.

Olson, J., Pollard, D.D., 1981. Inferring paleostresses from natural fracture patterns: a new method. Geology 17 (4), 345–348.

Oviatt, C.G., 1988. Evidence for Quaternary deformation in the Salt Valley Anticline, southeastern Utah. In: Doelling, H.H., Oviatt, C.G., Huntoon, P.W. (Eds.), Salt Deformation in the Paradox Region. Utah Geological and Mineral Survey, Salt Lake City, UT. Bulletin 122, pp. 61–78.

Peacock, D.C.P., 2001. The temporal relationships between joints and faults. Journal of Structural Geology 23, 329–341.

Pevear, D.R., Vrolijk, P.J., Lomgstaffe, F.J., 1997. Timing of Moab Fault displacement and fluid movement integrated with burial history using radiogenic and stable isotopes. In: Geofluids II Extended Abstracts, pp. 42–45.

Peng, S., Johnson, A.M., 1972. Crack growth and faulting in cylindrical specimens of Chelmsford granite. International Journal of Rock Mechanics and Mining Sciences 9 (1), 37–86.

Pollard, D.D., Aydin, A., 1988. Progress in understanding jointing over the past century. Geological Society of America Bulletin 100 (8), 1181–1204.

Rawnsley, K.D., Rives, T., Petit, J.-P., Hencher, S.R., Lumsden, A.C., 1992. Joint development in perturbed stress fields near faults. Journal of Structural Geology 14, 939–951.

Roznovsky, T.A., Aydin, A., 2001. Concentration of shearing deformation related to changes in strike of monoclinal fold axes: The Waterpocket monocline, Utah. Journal of Structural Geology 23, 1567–1579.

Scholz, C.H., Dawers, N.H., Yu, J.Z., Anders, M.H., 1993. Fault growth and fault scaling laws: preliminary results. Journal of Geophysical Research 98, 21951–21961.

Segall, P., Pollard, D.D., 1980. Mechanics of discontinuous faults. Journal of Geophysical Research 85 (8), 4337–4350.

Segall, P., Pollard, D.D., 1983. Nucleation and growth of strike slip faults in granite. JGR, Journal of Geophysical Research 88 (1), 555–568.

Shipton, Z.K., Cowie, P.A., 2001. Damage zone and slip surface-evolution over μm to km scales in high-porosity Navajo sandstone, Utah. Journal of Structural Geology 23, 1825–1844.

Taylor, W.L., Pollard, D.D., Aydin, A., 1999. Fluid flow in discrete joint sets: field observations and numerical simulations. Journal of Geophysical Research 104, 28983–29006.

Vrolijk, P., van der Pluijm, B.A., Treagus, S.H., 1999. Clay gouge. Questions in structural geology; 20th anniversary special issue. Journal of Structural Geology 21 (8–9), 1039–1048.

Wilkins, S.J., Gross, M.R., Wacker, M., Eyal, Y., Engelder, T., 2001.

Faulted joints: kinematics, displacement–length scaling relationships and criteria for their identification. Journal of Structural Geology 23, 315–327.

Willemse, E.J.M., Pollard, D.D., 1998. On the orientation and patterns of wing cracks and solution surfaces at the tips of a sliding flaw or fault. Journal of Geophysical Research 103 (2), 2427–2438.

Wong, T.-f., David, C., Zhu, W., 1997. The transition from brittle faulting to cataclastic flow in porous sandstones: mechanical deformation. Journal of Geophysical Research 102 (2), 3009–3025.

Zhao, G., Johnson, A.M., 1992. Sequence of deformations recorded in joints and faults, Arches National Park, Utah. Journal of Structural Geology 14 (2), 225–236.